Interaction Between Inclusions Embedded in Membranes

H. Aranda-Espinoza,*# A. Berman,§ N. Dan,¶ P. Pincus,‖ and S. Safran**

*Instituto de Física, Universidad Autónoma de San Luis Potosí, 78000 San Luis Potosí, S. L. P., Mexico; #Materials Research Laboratory and §Department of Chemical and Nuclear Engineering, University of California, Santa Barbara, California 93106-5080 USA; ¶Department of Chemical Engineering, University of Delaware, Newark, Delaware 19716 USA; ‖Departments of Materials and Physics, University of California, Santa Barbara, California 93106-5080 USA; and **Department of Materials and Interfaces, Weizmann Institute of Science, Rehovot 76100 Israel

ABSTRACT We calculate the membrane-induced interaction between inclusions, in terms of the membrane stretching and bending moduli and the spontaneous curvature. We find that the membrane-induced interaction between inclusions varies nonmonotonically as a function of the inclusion spacing. The location of the energy minimum depends on the spontaneous curvature and the membrane perturbation decay length, where the latter is set by the membrane moduli. The membrane perturbation energy increases with the inclusion radius. The Ornstein-Zernike theory, with the Percus-Yevick closure, is used to calculate the radial distribution function of inclusions. We find that when the spontaneous curvature is zero, the interaction between inclusions due to the membrane deformation is qualitatively similar to the hard-core interaction. However, in the case of finite spontaneous curvature, the effective interaction is dramatically modified.

INTRODUCTION

The properties of self-assembled bilayers dominate various systems such as vesicles, lyotropic liquid crystals, and block copolymer microstructures (Bloom et al., 1991; Abney and Owicki, 1985; Nelson et al., 1989; Safran et al., 1990; Sackmann, 1994; Fattal and Ben-Shaul, 1993). Perhaps the most interesting and important manifestation of amphiphilic bilayers is in the lipid membranes of biological systems. Although any single biomembrane may contain over 100 different lipids (Gennis, 1989), its behavior can be characterized by a small number of parameters that describe the free energy of deformation (Safran, 1994). Membranes also contain a variety of proteins that act as the active components and provide a diversity of biofunctions (Gennis, 1989). Proteins can be either adsorbed on the membrane surface or embedded in the bilayer. In the former case, the proteins may distort the packing of amphiphiles in one of the monolayers of the bilayer, whereas in the latter case the protein usually perturbs the equilibrium thickness of both monolayers (see Fig. 1, *top*).

In this paper we focus on the effect of embedded proteins on membrane structure and on the ensuing membrane-induced interaction between them. A number of biomembrane studies have investigated different aspects of this problem. Lewis and Engelman (1983) used freeze-fracture experiments to examine the effect of membrane thickness on the ordering of embedded proteins. They found that bacteriorhodopsin (protein) is dispersed in phosphatidylcholine bilayers, the thicknesses of which can be varied in the range of 1.95 to 3.45 nm by changing the lipid chain length; these thicknesses are from 1 nm thinner to 0.4 nm thicker than the protein hydrophobic surface. The proteins aggregate at bilayer thicknesses of 1.55 and 3.75 nm where the mismatch between membrane and protein thickness is significant. Measurements of the radial distribution function of bacteriorhodopsin (Lewis and Engelman, 1983) and rhodopsin (Chen and Hubbell, 1973) recombinants with diacyl phosphatidylcholine (PC) were compared with those calculated from liquid theory, using either a hard-disk repulsion or a hard-disk plus electrostatic repulsion interaction between particles (proteins) (Pearson et al., 1983). They indicated that bacteriorhodopsin in di 12:0, di 14:0, and di 16:0 PC bilayers interact as a hard-disk potential. Bleached rhodopsin in di 12:0 PC and di 18:1 *trans*-PC and dark-adapted rhodopsin in di 10:0 PC, besides the hard-disk repulsion, have an extra repulsion interaction, which was modeled as an electrostatic repulsion. The dark-adapted rhodopsin in di 18:1 *trans*-PC shows the evidence for an additional attractive interaction, which the authors propose is lipid mediated. Similarly, Pearson et al. (1984) calculated the pair distribution function of inclusions embedded in membranes using a thermodynamic model of the lipids, where the lipid-mediated force is approximated by its mean value. Comparing their results with the measurements done for *Acholeplasma laidlawii* (James and Branton, 1973) showed only slight differences between the predicted, theoretical, and experimentally observed pair distribution functions.

The first theoretical studies addressing the (lipid-mediated) interaction between inclusions were carried out taking into account two modes of membrane distortion: variations in thickness and in the surface area per amphiphile. These contribute both a compression-expansion and a surface tension term (Marčelja, 1976; Owicki and McConnell, 1979) to the free energy. The membrane thickness was found to decay exponentially from the inclusion-imposed value to the equilibrium membrane thickness, and the short-range membrane-induced interaction was predicted to be monotonically attractive.

Received for publication 12 February 1996 and in final form 16 May 1996.

Address reprint requests to Dr. Helim Aranda-Espinoza, Department of Physics, University of California, Santa Barbara, CA 93106-5080. Tel.: 805-893-8689; Fax: 805-893-2902; E-mail: helim@sbphy.physics.ucsb.edu.

0006-3495/96/08/648/09 $2.00

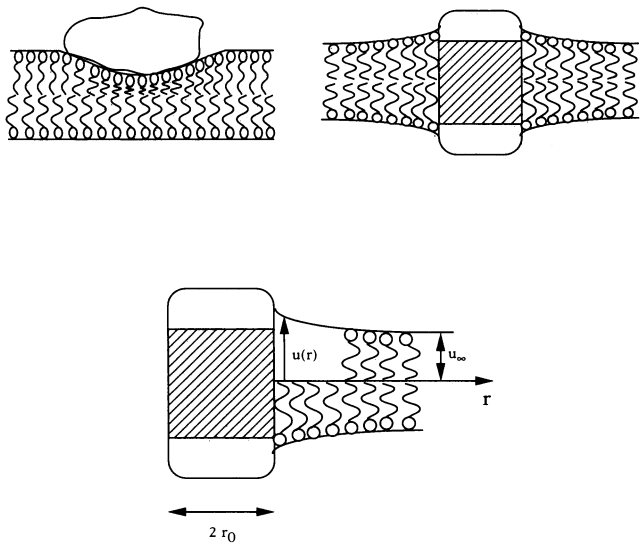

FIGURE 1 (*Top*) The protein distorts the membrane in two ways: adsorption, where only one monolayer is perturbed, and absorption, where the whole membrane is perturbed, i.e., the two monolayers are distorted. (*Bottom*) Profile of the *XY* plane. Some of the parameters that characterize the protein-bilayer system are shown: the radius of the inclusion, r_0, the equilibrium flat layer thickness, u_∞, and the thickness of the membrane as a function of the distance from the center of the inclusion, $u(r)$.

Elliot et al. (1983) investigated the lifetime of gramicidin single channels embedded in monoacylglycerol bilayers. Their measurements indicated that the increase in bilayer thickness reduced the mean channel lifetime. They proposed a theoretical model that related the mean channel lifetime to both the thickness and the tension of the bilayer. In their model the gramicidin channel is modeled as a dimer; the distorted bilayer pulls the gramicidin in such a way that it breaks the dimer (so the channel stops its ion-conducting function). To fit the experimental data, the model required that the bilayer pull the proteins a distance of 1.8 nm apart. This distance is much larger than what could be expected from the rupture of hydrogen bonds.

The shortcomings of the analysis by Elliot et al. (1983) were remedied by Huang (1986), who used the free energy expression for the distortion of a smectic liquid crystal to describe the perturbed membrane and to calculate the properties of these embedded gramicidin channels. The energy, in this model, consists of not only the compression term and surface tension terms, but also of a splay, or bending term. Proposing that the membrane pull on the gramicidin dimer is much weaker (0.1 nm) yielded excellent agreement with the results of Elliot et al. (1983). Thus, Huang's calculation indicated that the bending (splay) energy plays a significant role in determining the membrane-induced interactions. It is also interesting to note that Huang's (1986) numerical results indicated that the membrane thickness, rather than decaying exponentially from the gramicidin boundary to the equilibrium value (Marčelja, 1976; Owicki and McConnell, 1979), is nonmonotonic. Helfrich and Jakobsson (1990) extended Huang's work to show that the surface tension makes a small contribution to the free energy when the membrane is thin and not solvent-containing.

Using the smectic liquid crystal model, Goulian et al. (1993) and Palmer et al. (1994) calculated the interactions between rigid inclusions (as a generic model for proteins) embedded in membranes. Keeping only the bending term and neglecting both the compression and surface contributions, they predicted nonmonotonic interactions as a function of the distance between inclusions; at large separations the interaction between similar inclusions was found to be a weak attractive power law of the distance between inclusions. In single bilayer systems, or in cases where the separation between inclusions is much smaller than the layer spacing so that the presence of the other membranes is screened, the interaction was found to scale as the inverse of the fourth power of the distance between inclusions.

Most models concentrated on the interactions between two isolated inclusions. However, in biosystems the concentration of proteins is, as a rule, high (Gennis, 1989), so that protein interaction is a many-body problem. Dan et al. (1994) investigated the perturbation profile and the membrane-induced interaction between inclusions ordered in a Wigner-Seitz cell (the cell formed by the perpendicular bisectors of the vectors between the inclusion and all its nearest neighbors). Balancing the compression-expansion term with the bending contribution, it was found that the membrane thickness profile decays nonmonotonically as a function of distance from the inclusion boundary. Although the perturbation decay length agreed with Huang's (1986) predictions, the profiles obtained in the two models differed, because of the use of different boundary conditions. The membrane-induced interactions between inclusions were found to be attractive when the membrane thickness was constrained to match an inclusion-imposed value, as predicted by Marčelja (1976) and Owicki and McConnell (1979). However, unlike the earlier studies, accounting for the bending energy gave rise to an energy barrier in the energy versus separation between inclusions. This barrier could promote a metastable state characterized by a definite spacing between inclusions. In systems where the membrane was constrained to meet the inclusion at a finite contact angle, the short-range membrane-induced interaction was found to be strongly repulsive. The equilibrium state was predicted, in this case, to be an array of inclusions at a definite spacing (Dan et al., 1994).

All of these models neglect the spontaneous curvature of the membrane (Helfrich, 1973), which describes the tendency and magnitude of an amphiphile monolayer to curve at the water/oil interface. The role of spontaneous curvature was usually ignored because the symmetry between the two monolayers composing the bilayer excludes curvature (Safran, 1994; Helfrich, 1973; Israelachvili, 1992), so that the equilibrium bilayer adopts a locally flat configuration. Dan et al. (1993) calculated the perturbation profile and the membrane-induced interaction between embedded inclusions, taking into account not only the compression-expansion, and the bending energies, but also the effect of the spontaneous curvature of each monolayer of the bilayer. Using a one-dimensional model (namely, where the inclusion thickness was assumed to be much larger than the

membrane correlation length), they found that the inclusions decouple the two monolayers composing the bilayer. As a result, the sign and magnitude of the amphiphile's spontaneous curvature dominate both the membrane perturbation profile and the membrane-induced interaction between inclusions. The membrane profile was shown to always oscillate as a function of distance from the inclusion boundary, with a periodicity that depends on the sign and magnitude of the spontaneous curvature. The type of interactions (whether attractive or repulsive), their range, and their magnitude varied with the spontaneous curvature and the inclusion-imposed boundary condition. Recently, Kralchevsky et al. (1995) used a "sandwich model" to calculate the perturbation profile, the interaction energy, and the lateral capillary force between two isolated inclusions. The phenomenological parameters used in their "sandwich model" were shown to relate to the Helfrich parameters (1973), specifically, the bending energy and spontaneous curvature. Assuming high surface tension of the flat bilayer (whereas Dan et al., 1993, take it to be zero), they found an exponentially decaying perturbation profile, and nonmonotonic lateral capillary force and interaction between the two inclusions.

In this paper we use a similar (Dan et al., 1993, 1994) approach to calculate the membrane perturbation profile and the membrane-induced interaction between an array of inclusions embedded in a two-dimensional membrane. This interaction is then used to predict the radial distribution function of inclusions in the membrane using a calculation based on liquid state theory.

We find that the thickness profile of the membrane oscillates around the inclusion, decaying to the flat membrane thickness at a large distance from the inclusion boundary. The membrane-induced interaction between inclusions decays nonmonotonically with the distance between them. Depending on the parameters that characterize the system (spontaneous curvature, stiffness, radius of the inclusion, etc.), the membrane can promote either aggregation or a finite spacing between inclusions. Likewise, our results suggest that there are metastable states where a finite spacing between inclusions is preferred. The energy penalty for inserting an inclusion in the membrane may be either negative or positive, depending on the system parameters. In the former case the membrane will prefer to absorb the inclusion, in the latter to reject it. As expected, our results show that increasing the radius of the inclusion increases the perturbation of the membrane. When the inclusion radius is greater than the membrane decay length, the inclusion can be taken to be a "one-dimensional" infinite wall (Dan et al., 1993).

The radial distribution function (RDF) gives a measure of the probability that two inclusions will be at a given spacing. Because the RDF can be obtained experimentally, it provides a way to verify the accuracy of a predicted potential (Pearson et al., 1983, 1984). In this paper we calculate the RDF of inclusions in membranes. We find that, for the parameters chosen, the interaction between inclusions is short-ranged and dominated by the spontaneous curvature of each monolayer of the bilayer. When the spontaneous curvature is zero, the RDF due to the membrane-induced interaction is nearly identical to that of a hard disk (because, in effect, this is a two-dimensional system) liquid. When the spontaneous curvature is nonzero, the RDF shows that a finite inclusion spacing is preferred. This spacing is similar to the distance at which the membrane-induced interaction energy between inclusions is minimal. Finally, we see that the decay of the oscillations of all the RDF shown in this work (hard-disk potential model, zero and finite spontaneous curvature) is approximately at the same distance, which implies that the membrane-induced interaction between inclusions is short-range for the parameters chosen in our analysis. These were chosen to roughly correspond to the experimental values of the monoacylglycerol-squalene and lecithin bilayers (Huang, 1986), so that the dimensionless values of the ratio between the compressibility and the bending moduli is 10 and the spontaneous curvature is 0.4.

THEORY

Consider a non-solvent-containing membrane that contains embedded inclusions that are arranged on an hexagonal lattice, so that each inclusion can be taken to be surrounded by its Wigner-Seitz cell. We simplify this by assuming radial symmetry. The inclusions can be either thicker or thinner than the equilibrium (unperturbed, flat) membrane thickness. A strong coupling, arising from the need to match the hydrophobic part of the membrane and the hydrophobic part of the inclusion to avoid contact with water, distorts the membrane thickness at the inclusion boundary. Assuming that the membrane is composed of one type of amphiphile, the system is symmetrical around the bilayer midline, and the inclusion-imposed deformation is identical for the two monolayers composing the bilayer. Then we need only consider the perturbation profile of a single monolayer (see Fig. 1, *bottom*). Taking the membrane to be parallel to the *X-Y* plane, and defining $u(r)$ as the thickness of the membrane, where r is the coordinate from the center of the inclusion (see Fig. 1, *bottom*), the free energy, per amphiphile, of a monolayer can be written as (Helfrich, 1973; Dan et al., 1993, 1994)

$$f(u,\Sigma) = f_0(\Sigma) + \kappa(\Sigma)\nabla^2 u + K(\Sigma)(\nabla^2 u)^2, \qquad (1)$$

where $\Sigma \equiv \Sigma(r)$ is the local surface area per amphiphile.

The local monolayer thickness, $u(r)$, is related to Σ by an equation of state. In this calculation, we use an incompressibility condition. Accounting for the effects of curvature,

$$v \approx u\Sigma\left[1 + \left(\frac{du}{dr}\right)^2\right]^{1/2}, \qquad (2)$$

where v is the volume per amphiphile. The free energy of a flat monolayer is given by $f_0(u, \Sigma) = \gamma\Sigma + G(u)$, where γ is the surface tension between the aqueous media and the hydrophobic amphiphile tails, and $G(u)$ the contribution to the energy of the compression-expansion term of the am-

phiphiles. $K(\Sigma)$ and $\kappa(\Sigma)/K(\Sigma)$ are the bending stiffness and spontaneous curvature per molecule, respectively. The local monolayer curvature is given by $\nabla^2 u$. We neglect the surface tension contribution to the energy, according to the results of Helfrich and Jakobsson (1990). All energies are given in units of k_BT, where k_B is the Boltzmann constant and T is the temperature.

An unperturbed, and thus, locally flat, membrane is characterized by a thickness u_∞ and area per amphiphile Σ_∞, which are determined by the minimization of the $f_0(u, \Sigma)$. Assuming that the perturbation of the membrane is small, the perturbation energy (per amphiphile) due to local curvature is given, to second order in curvature and surface area, by

$$\delta = f(\Sigma) - f_0 \approx (\Sigma - \Sigma_\infty)^2 f_0''/2 + \kappa\nabla^2 u + k'(\Sigma - \Sigma_\infty)\nabla^2 u + K(\nabla^2 u)^2, \quad (3)$$

where $f_0'' \equiv \partial^2 f_0/\partial\Sigma^2$ and $\kappa' \equiv \partial\kappa/\partial\Sigma$, evaluated at $\Sigma = \Sigma_\infty$ (throughout the paper we use the convention that the prime denotes $\partial/\partial\Sigma$, evaluated at Σ_∞), $K = K(\Sigma_\infty)$, and $\kappa = \kappa(\Sigma_\infty)$. Higher order terms were neglected in Eq. 3, because we assume that the local curvature is small. We define a dimensionless perturbation parameter, $\Delta(r)$, as the change in $u(r)$ relative to the unperturbed thickness of the membrane, u_∞,

$$\Delta(r) = (u(r) - u_\infty)/u_\infty \quad (4a)$$

$$\Sigma - \Sigma_\infty \approx -v\Delta/u_\infty, \quad (4b)$$

where Eq. 4b was obtained by use of the incompressibility condition (Eq. 2) and the assumption of small perturbation (so that $|\Delta(r)| \ll 1$).

The overall change in the membrane free energy, per inclusion, is equal to

$$F = \int_{r_0}^{r_0+L} dr 2\pi r \frac{Ku_\infty^3}{v}[\beta\Delta^2 + \delta\nabla^2\Delta + \lambda\Delta\nabla^2\Delta + (\nabla^2\Delta)^2], \quad (5)$$

where $\beta = B/2Ku_\infty^2$, $B = \Sigma_\infty^2 f_0''$ (stretching modulus), $\lambda = (\kappa - \Sigma_\infty\kappa')/Ku_\infty$, and $\delta = \kappa/2Ku_\infty$. The integration was done on a circular region of radius $r = r_o + L$, where r_o is the radius of the inclusion, $2L$ is the distance between two adjacent inclusion boundaries, and we have used Eqs. 4a and 4b. Once the perturbation profile $\Delta(r)$ is known, we can calculate the membrane-induced interaction between inclusions and compare the energetic contribution of the different terms (compression-expansion, bending stiffness, and spontaneous curvature).

Minimization of Eq. 5 with respect to variations in the perturbation profile $\Delta(r)$ yields the Euler-Lagrange equation:

$$\nabla^4\Delta + \lambda\nabla^2\Delta + \beta\Delta = 0. \quad (6)$$

The general solution of this Euler-Lagrange equation is given by

$$\Delta(r) = A_1 J_0(\alpha_1 r) + A_2 Y_0(\alpha_1 r) + A_3 J_0(\alpha_2 r) + A_4 Y_0(\alpha_2 r), \quad (7)$$

where $J_0(x)$ and $Y_0(x)$ are the zeroth-order Bessel functions of first and second kinds, respectively, $\alpha_1 = (\lambda + (\lambda^2 - 4\beta)^{1/2}/2)^{1/2}$ and $\alpha_2 = (\lambda - (\lambda^2 - 4\beta)^{1/2}/2)^{1/2}$. We can see from the functional form of Eq. 7 that α_1 and α_2 set the length scale at which the perturbation profile decays, namely, the decay length of the membrane. The value of these parameters depends on the physical properties of the membrane as given by λ and β. The constants A_i are determined by the boundary conditions. These include the thickness-matching condition, $\Delta(r_o) = \Delta_0$, where Δ_0 defines the size of the hydrophobic inclusion region. The second boundary condition is given by symmetry, $d\Delta(r)/dr = 0$ at the midpoint between inclusions, $r = r_o + L$. The two remaining boundary conditions are given by the minimization requirements of Eq. 5,

$$\nabla^3\Delta \,|_{r=r_0+L} = 0, \quad (8)$$

where $\nabla^3 = d/dr(1/r \cdot d/dr(r \cdot d/dr))$, and

$$\nabla^2\Delta \,|_{r=r_0} = -\delta - \lambda/2. \quad (9)$$

We can obtain a simple expression for the inclusion-imposed energy by integrating by parts the second and the last terms (twice) in the right-hand side of Eq. 5, using the Euler-Lagrange equation (Eq. 6) and the respective boundary conditions. Thus, we find that the energy in the thickness-matching boundary condition system is

$$F_T \equiv \frac{vF}{2\pi r_0 K} = \left(\left(\frac{\Delta_0\lambda}{2} - \delta\right)\left(\frac{d\Delta}{dr}\right) + \Delta_0(\nabla^3\Delta)\right)_{r=r_0}. \quad (10)$$

Once we have computed the free energy of the system (Eq. 10) we can calculate the RDF of inclusions in the membrane. To do this, we need to know the interaction between inclusions. The free energy, Eq. 10, gives us the penalty energy of the incorporation of one inclusion plus the cost of adding another inclusion once we have one inclusion in the membrane; because our model is not considering three (or more) body interactions, we can subtract the penalty energy due to the incorporation of a single inclusion from the energy in Eq. 10, and in doing this we will get the net membrane-induced interaction between inclusions, which we will denote as

$$V(r) = F_T - F_{T\infty}, \quad (11)$$

where $F_{T\infty}$ is the free energy when $L/u_\infty \to \infty$, thereby denoting the membrane-induced "absorption" energy of a single inclusion.

We use the Ornstein-Zernike integral equation to calcu-

late the RDF, given by

$$g(r) = 1 + c(r) + \rho \int c(\mathbf{r}')(g(\mathbf{r} - \mathbf{r}') - 1)\mathrm{d}^2r', \quad (12)$$

where $g(r)$ is the radial distribution function, $c(r)$ is the direct correlation function, and ρ is the density of inclusions in the membrane. To solve this equation we need another relationship between $c(r)$ and $g(r)$. We use the Percus-Yevick closure, which is a good approximation for short-range interactions (Hansen and McDonald, 1986),

$$c(r) = g(r)(1 - e^{\omega(r)/\kappa_B T}), \quad (13)$$

where $w(r)$ is the interaction potential between inclusions; in this paper we will use a hard-disk potential plus the potential in Eq. 11. We will follow the method given by Lado (1968) to solve Eqs. 12 and 13, thereby finding the distribution of inclusions.

RESULTS

Membrane properties are defined by the parameters δ, λ, and β. The first characterizes the amphiphile spontaneous curvature, and thus, the frustration of the monolayer inherent in the equilibrium, flat bilayer configuration. The second accounts for the variation of the spontaneous curvature with respect to the change in the surface amphiphile density. The last parameter quantifies the ratio between the stretching and bending moduli of the monolayer. When β is small, the energy required for a bending deformation is much higher than the penalty incurred by compression/expansion of the monolayer, and vice versa. δ, λ, and β thus determine the characteristics of the inclusion-induced thickness perturbation profile, the ensuing membrane-induced interaction between inclusions, and the radial distribution function of inclusions in the membrane.

For simplicity, we use the same set of membrane parameters throughout the paper. The value of β is 10, and $\Delta_0 = 0.05$. When noninteracting inclusions are discussed, the distance between inclusions is taken to be $L/u_\infty = 10$; such a distance is sufficient to exclude interactions between neighboring inclusions, i.e., overlap of the perturbed regions. To establish the role of spontaneous curvature, we examine three different cases: $\delta = 0.4$, 0, and -0.4, which correspond to $\lambda = 0.1$, 0, and -0.1, respectively. The decay length is defined by the real part of α_1 (which is equal to the real part of α_2) and is approximately equal to $1.3u_\infty$.

In Fig. 2 we plot the thickness profile surrounding a single inclusion, as a function of distance from the inclusion boundary. The inclusion radius is equal to u_∞. We see that the thickness perturbation profile strongly depends on the spontaneous curvature value of the monolayer. When δ is small, the profile resembles an exponentially decaying function; oscillations are discernible only by a shallow minimum in the thickness at a reduced distance of about $2u_\infty$. The value of $\Delta(r)$ decreases, at that point, below zero, i.e., the thickness of the membrane in this region is smaller than that of the equilibrium, flat membrane. This is in agreement with previous calculations (Huang, 1986; Dan et al., 1994) where the spontaneous curvature of the monolayer was neglected. When the value of δ is large, the oscillations in the thickness profile are more pronounced. The sign of δ defines the tendency of the monolayer to curve to, or from, the water/oil interface; as a result, systems with positive δ "overshoot" so as to simulate a positive curvature, whereas systems with a negative value of δ "undershoot." These results are in qualitative agreement with the calculations by Dan et al. (1993), where the inclusions were taken to be large (i.e., $r_0 \to \infty$).

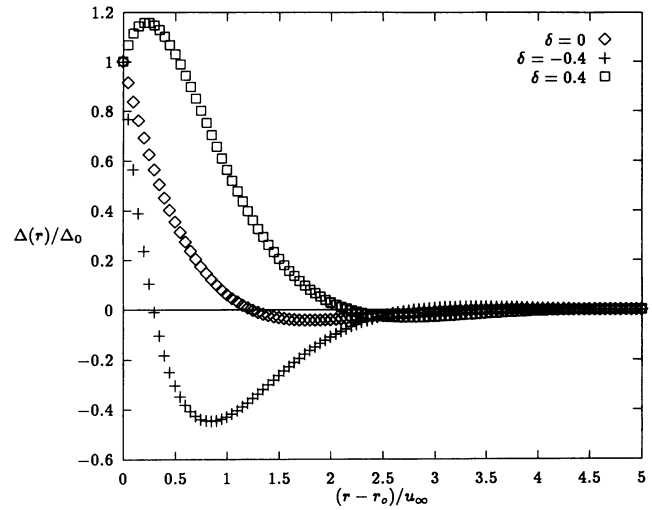

FIGURE 2 Perturbation profiles as a function of the distance from the inclusion boundary for different values of the spontaneous curvature of the monolayer, δ. The distance between inclusions is $L/u_\infty = 10$, the thickness-matching boundary condition is $\Delta_0 = 0.05$, the dimensionless radius of the inclusion is $r_o/u_\infty = 1$, the ratio between the monolayer bending and the stretching moduli is $\beta = 10$, and $\lambda = 0$, -0.1, 0.1 when $\delta = 0$, -0.4, 0.4 respectively.

The energetic difference between the membrane-perturbed and the equilibrium, flat membrane, F_T, is plotted in Fig. 3 as a function of the separation between inclusions, L/u_∞, for the three systems depicted in Fig. 2. We see that when the spontaneous curvature is zero, the energetic minimum is obtained at $L/u_\infty = 0$. This indicates that, in such a system, the membrane-induced interactions drive the inclusions to aggregate. However, a barrier to aggregation exists in the form of an energy maximum at $L/u_\infty \approx 1$. This barrier could promote a metastable state characterized by the secondary minimum, so that the inclusions will order with a finite separation between them. This is in agreement with the calculations of Dan et al. (1994) for inclusions embedded in membranes of zero spontaneous curvature of each monolayer of the bilayer. When the spontaneous curvature is nonzero, aggregation of inclusions is unfavorable. Rather, the system's energy is minimal when the inclusions adopt a specific spacing. Note that when $\delta = 0.4$ an energy barrier might, as in the zero spontaneous curvature case, promote a meta-stable state characterized by the secondary minimum. This is a feature of the two-dimensional system that was not found in the one-dimensional case.

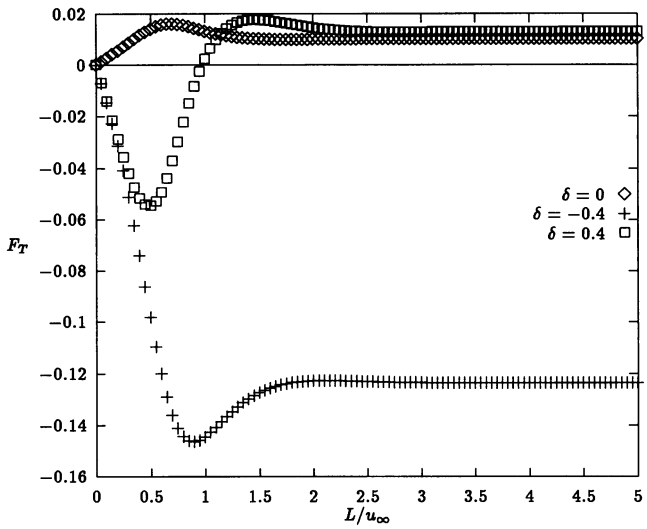

FIGURE 3 The dimensionless free energy as a function of the distance between inclusions. The parameters are the same as in Fig. 2.

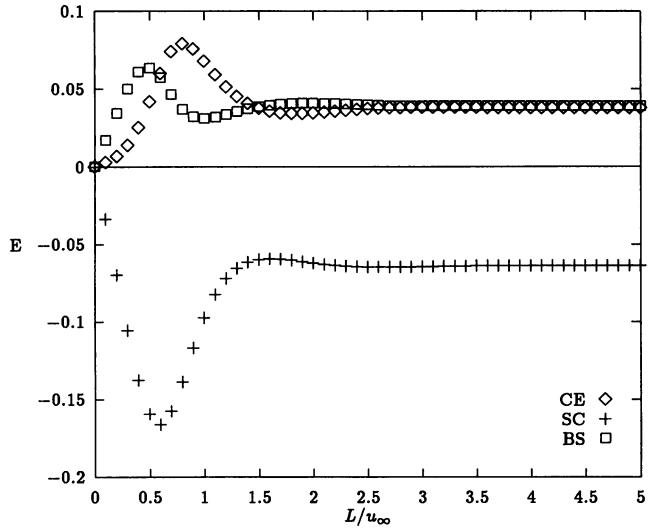

FIGURE 4 Decomposition of the different energy contributions. Compression-expansion (CE), spontaneous curvature (SC), and bending stiffness (BS). Each term is in units of $2\pi r_o K/v$. The radius of the inclusion is $r_o/u_\infty = 1$, the distance between inclusions is $L/u_\infty = 10$, and the thickness-matching boundary condition is $\Delta_0 = 0.05$. The spontaneous curvature of the monolayer is $\delta = 0.4$, the ratio between the monolayer bending and the stretching moduli is $\beta = 10$, and $\lambda = 0.1$.

The value of F_T in the limit of $L/u_\infty \to \infty$ defines the energy gained, or lost, due to incorporation of a single inclusion in the membrane. When $\delta = 0$ or $\delta = 0.4$, the membrane will tend to reject the inclusion.

When $\delta = -0.4$ the membrane energy is reduced by the inclusion, in agreement with the predictions of Dan et al. (1993). Figs. 2 and 3 show the effect of the spontaneous curvature in determining the profile and the membrane-induced energy between inclusions. Decomposition of the membrane energy shows more clearly, however, the weight of each contribution: the compression/expansion term, the spontaneous curvature term, and the bending stiffness term. In Fig. 4 the three contributions are shown (using Eq. 5) as a function of the distance between inclusions. The values of λ and δ are 0.1 and 0.4, respectively. We see that the predominant energetic contribution is that due to the spontaneous curvature of the monolayer, δ. The relative importance of the bending and the compression/expansion terms are set by the value of $\beta \propto B/K$; in this case we chose a high ratio whereby the bending stiffness is smaller and less important than the compression/expansion contribution. A similar conclusion is reached for a system when the spontaneous curvature is -0.4.

The inclusion size influences the membrane perturbation profile and energy. In general, we expect that larger inclusions perturb a larger area of the membrane and thus have a stronger effect than smaller inclusions. In the limit where the inclusion radius is larger than the membrane perturbation decay length, the system will resemble the one-dimensional ("infinite wall-like") inclusions discussed by Dan et al. (1993). The effect of inclusion radius on the monolayer thickness profile is shown in Fig. 5 for a system with positive spontaneous curvature (the same analysis is valid for systems with zero and negative spontaneous curvature). We see that the inclusion radius does not significantly affect the perturbation profile. Only the magnitude of the first thickness "overshoot" decreases slightly with inclusion radius. One might therefore expect that the membrane energy (as a function of the spacing between inclusions) will also be unaffected. Indeed, as can be seen in Fig. 6, the location of the energy minimum, which defines the energetically optimal spac-

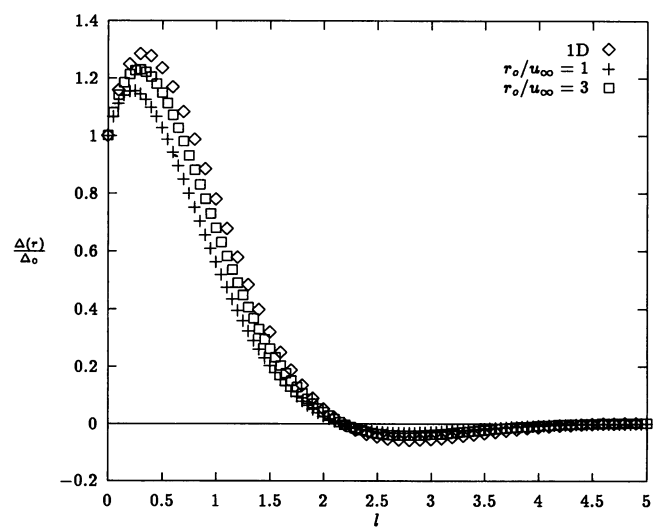

FIGURE 5 Perturbation profile as a function of the distance from the inclusion boundary for a one-dimensional system (◇), the two-dimensional system with the radius of the inclusion $r_o/u_\infty = 1$ (+), and radius of $r_o/u_\infty = 3$ (□). The parameters are the same as in Fig. 4. For the one-dimensional system $l \equiv r/u_\infty$, and for the two-dimensional case $l \equiv (r - r_o)/u_\infty$.

ing, is unaffected by the inclusion radius. So, to a large extent, is the depth of the energy minimum. However, the membrane perturbation energy at large inclusion spacings varies significantly with the inclusion radius.

As mentioned earlier, the value of F (or E) in the limit of $L \rightarrow \infty$ defines the effective membrane-induced inclusion absorption energy. Therefore, whereas small inclusions will be rejected by the membrane at small concentrations, large inclusions will be readily absorbed.

It is of interest to estimate the magnitude of the membrane-induced interaction energy. The energy is given (Eq. 10) in units of $2\pi K r_o/v$, which, for gramicidin channel (Huang, 1986), is 6.2×10^{-13} erg. For comparison, at $T = 300$K, $k_B T = 4.1 \times 10^{-14}$ erg. Therefore, when the inclusion-induced perturbation is large, namely, Δ_0 is large, the membrane-induced interaction between inclusions will be on the same order of magnitude as $k_B T$.

The radial distribution function, $g(r)$, gives a measure of the probability that two inclusions will be at a distance r from each other (Hansen and McDonald, 1986). The mean spacing is, therefore, approximately given by the location of the first peak. In Fig. 7 we compare the RDF of inclusions embedded in membranes of several spontaneous curvatures to that of a hard-disk liquid. We see that, for the parameters chosen in this paper, the RDF of inclusions in a membrane with zero spontaneous curvature is practically identical to that of a two-dimensional fluid with hard-disk interaction. As could be expected from the energy profile, the average spacing between inclusions is unity, corresponding to an aggregated state. However, in membranes of finite spontaneous curvature of the monolayer, this is not the case. The maximum occurs at a definite value, which corresponds, approximately, to the location of the energy minimum (as shown in Fig. 3. Note that in our notation $r = r_o + L$). We see that, at spacings larger than $r/u_\infty \approx 3$, $g(r)$ decays to unity. This indicates that the membrane-induced interaction is very short-range. However, this is due to our choice of parameters, namely, the correlation length is approximately equal to the membrane thickness u_∞. In systems with larger correlation lengths the interaction range will be longer.

CONCLUSIONS

In this paper the properties of membranes containing embedded inclusions are calculated as a function of membrane parameters and inclusion size. The two-dimensional model used allows investigation of the membrane perturbation profile, the membrane-induced interaction between inclusions, and their radial distribution function. The shape of the membrane deformation profile, as a function of distance from the inclusion boundary, strongly depends on the spontaneous curvature of the monolayers. The elastic properties of the membrane, namely, compressibility and bending energy, set the perturbation decay length. This decay length defines both the distance from the inclusion at which the equilibrium thickness is reached (if the inclusions are widely spaced), and the radius of the inclusion above which a simplified one-dimensional model applies.

The perturbation profile was used to calculate the membrane energy. We find that the energy gain, or loss, due to absorption of an inclusion in the membrane, is set by the spontaneous curvature of each monolayer of the bilayer. For the parameters chosen, in systems of zero and positive spontaneous curvature of the monolayer, the membrane energy increases because of inclusion absorption, thereby inhibiting absorption. On the other hand, the energy of a

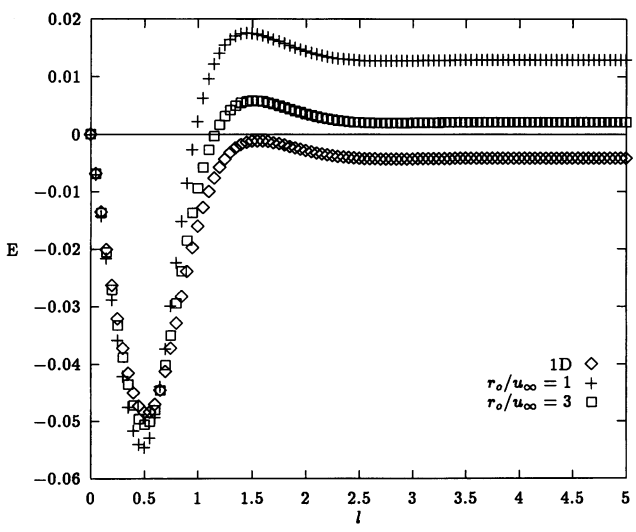

FIGURE 6 Comparison of the free energy between systems in the one- and the two-dimensional models. The parameters and l are as in Fig. 5. $E \equiv vF/K$ for the one-dimensional system, where F is the energy per unit inclusion width, and $E \equiv vF/2\pi r_o K$ for the two-dimensional system.

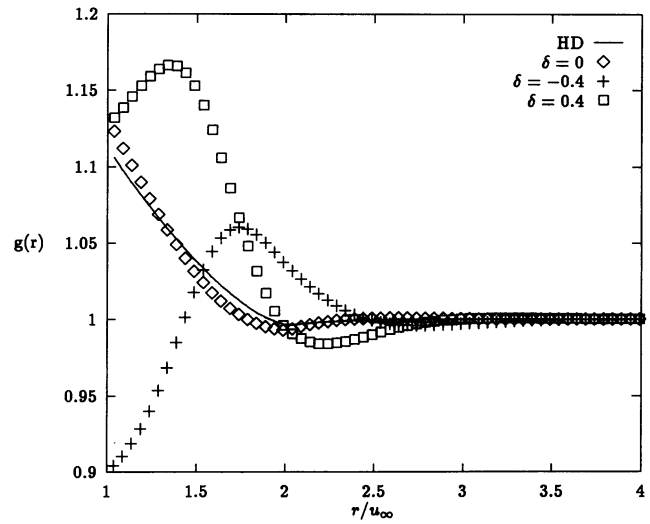

FIGURE 7 Radial distribution functions as a function of the distance between centers of the inclusions, for a reduced density $\rho^* \equiv 4\rho r_o^2 = 0.08$. The membrane and inclusion parameters are as in Fig. 2. A comparison is made between a hard-disk potential liquid model (solid line) and membranes with different values for the spontaneous curvature of each monolayer of the bilayer, $\delta = 0$ (◇), $\delta = -0.4$ (□), and $\delta = 0.4$ (+).

membrane with negative spontaneous curvature of the monolayer is reduced by inclusions, thus promoting inclusion absorption. These effects on the membrane energy are due to the fact that the inclusion distorts the membrane in such a way that the distortion either can or cannot fit the spontaneous curvature of each monolayer of the bilayer.

The membrane-induced interactions between inclusions are nonmonotonic; the presence of energy barriers could lead to metastable states characterized by an inclusion spacing other than that of the equilibrium minimum free energy. For membranes where each monolayer has zero spontaneous curvature, the energy is minimal when the inclusions are aggregated. In systems of finite spontaneous curvature the preferred state is that of inclusions distributed at a specific spacing. This spacing allows the membrane to deform in such a manner consistent with both, the inclusion deformation and the intrinsic spontaneous curvature of each monolayer.

These effects on the perturbation profile and on the membrane-induced interaction between inclusions are due to the fact that the inclusion distorts the membrane in such a way that the distortion either can or cannot fit the spontaneous curvature of each monolayer of the bilayer. For example, for the parameters chosen in this paper, the inclusion forces the membrane to deform in such a manner that a negative spontaneous curvature of the monolayer would be favorable (see Fig. 3).

An interesting effect is observed when the spontaneous curvature of the monolayer is positive. For short distances between inclusions the energy is decreased, indicating that absorption is favorable for this configuration. This is due to the coupling between the distortion of the inclusions on the membrane and the spontaneous curvature as indicated above. In this case for short distances the monolayer "overshoots" so as to simulate a positive curvature (see Fig. 2), and therefore, the energy is decreased. Examining the various energetic contributions, we find that the membrane deformation energy is dominated by the spontaneous curvature of the monolayers. This conclusion is, however, parameter dependent. In membranes where the bending stiffness or compressibility is very high, the spontaneous curvature will play a less important role. The spontaneous curvature also determines how the inclusion size affects the system energy. The membrane energy can either increase or decrease with inclusion radius, depending on the various system parameters. However, the results of a simplified one-dimensional model (Dan et al., 1993) are recovered when the inclusion radius is larger than the membrane decay length.

The membrane-induced interaction between inclusions was used to compute the RDF. The mean distance between inclusions, as defined by the first peak in the RDF, is similar to that given by the location of the membrane energy minimum. The RDF of inclusions in membranes of zero spontaneous curvature is similar to that of a hard-disk liquid. The membrane-induced interactions are found to be short-range for the parameters we investigate. Longer range interactions are possible in cases where the membrane decay length is larger (e.g., for smaller bending modulus K).

Unfortunately, we cannot yet examine the validity of our predictions by comparison with experimental data. We do not know of experiments where the spacing of inclusions, as well as all the necessary parameters (compressibility, spontaneous curvature, bending modulus) have been measured. Moreover, in many experimental systems the electrostatic interactions between inclusions (proteins) need to be included. However, this model represents another step in the effort to understand and characterize the interactions between embedded inclusions. Refining the model so that it will be more applicable includes adding the direct inclusion-inclusion interactions (van der Waals and electrostatic) (Dan and Safran, manuscript in preparation). Furthermore, the Ornstein-Zernike theory we use to calculate the RDF applies to flat surfaces, although membranes are known to undulate and curve. Therefore, it is of interest to extend the model to calculate the distribution function for curved and fluctuating membranes (Aranda-Espinoza and Pincus, manuscript in preparation).

HAE and PP acknowledge the support of the National Science Foundation, grant DMR-9301199, and the Materials Research Laboratory at UCSB, supported by NSF grant DMR-9123048. HAE also acknowledges the support of the Consejo Nacional de Ciencia y Tecnologá. ND acknowledges the support of the AAUW.

REFERENCES

Abney, J. R., and J. C. Owicki. 1985. Theories of protein-lipid and protein-protein interactions in membranes. *In* Progress in Protein-lipid Interactions. A. Watts and J. De Pont, editors. Elsevier, New York.

Bloom, M., E. Evans, and O. G. Mouritsen. 1991. Physical properties of the lipid-bilayer component of cell membranes—a perspective. *Q. Rev. Biophys.* 11:293–397.

Chen, Y. S., and W. L. Hubbell. 1973. Temperature- and light-dependent structural changes in rhodopsin-lipid membranes. *Exp. Eye Res.* 17: 517–532.

Dan, N., A. Berman, P. Pincus, and S. A. Safran. 1994. Membrane-induced interactions between inclusions. *J. Phys. II France.* 4:1713–1725.

Dan, N., P. Pincus, and S. A. Safran. 1993. Membrane-induced interactions between inclusions. *Langmuir.* 9:2768–2771.

Elliot, J. R., D. Needham, J. P. Dilger, and D. A. Hayden. 1983. The effects of bilayer thickness and tension on gramicidin single-channel lifetime. *Biochim. Biophys. Acta.* 735:95–103.

Fattal, D. R., and A. Ben-Shaul. 1993. A molecular model for lipid-protein interaction in membranes: the role of hydrophobic mismatch. *Biophys. J.* 65:1795–1809.

Gennis, R. B. 1989. Biomembranes: Molecular Structure and Functions. Springer Verlag, New York.

Goulian, M., R. Bruinsma, and P. Pincus. 1993. Long-range forces: in heterogeneous fluid membranes. *Europhys. Lett.* 22:145–150.

Hansen, J. P., and I. R. McDonald. 1986. Theory of Simple Liquids, 2nd Ed. Academic, New York.

Helfrich, W. 1973. Elastic properties of lipid bilayers: theory and possible experiments. *Z. Naturforsch.* 28C:693–703.

Helfrich, P., and E. Jakobsson. 1990. Calculation of deformation energies and conformations in lipid membranes containing gramicidin channels. *Biophys. J.* 57:1075–1084.

Huang, H. W. 1986. Deformation free energy of bilayer membrane and its effects on gramicidin channel lifetime. *Biophys. J.* 50:1061–1070.

Israelachvili, J. 1992. Intramolecular and Surface Forces, 2nd Ed. Academic Press, London.

James, R., and D. Branton. 1973. Lipid- and temperature-dependent structural changes in *Acholeplasma laidlawii* cell membranes. *Biochim. Biophys. Acta.* 323:378–390.

Kralchevsky, P. A., V. N. Paunov, N. D. Denkov, and K. Nagayama. 1995. Stresses in lipid membranes and interactions between inclusions. *J. Chem. Soc. Faraday Trans.* 91:3415–3432.

Lado, F. 1968. Equation of state of the hard disk fluid from approximate integral equations. *J. Chem. Phys.* 49:3092–3096.

Lewis, B. A., and D. M. Engelman. 1983. Bacteriorhodopsin remains dispersed in fluid phospholipid bilayers over a wide range of bilayer thicknesses. *J. Mol. Biol.* 166:203–210.

Marčelja, S. 1976. Lipid-mediated protein interaction in membranes. *Biochim. Biophys. Acta.* 455:1–7.

Nelson, D., T. Piran, and S. Weinberg. 1989. Statistical Mechanics of Membranes and Surfaces. World Scientific, Singapore.

Netz, R., and P. Pincus. 1995. Inhomogeneous fluid membranes—segregation ordering and effective rigidity. *Phys. Rev. E.* 52:4114–4128.

Owicki, J. C., and H. M. McConnell. 1979. Theory of protein-lipid and protein-protein interactions in bilayer membranes. *Proc. Natl. Acad. Sci. USA.* 76:4750–4754.

Palmer, K. M., M. Goulian, and P. Pincus. 1994. Fluctuation-induced forces in stacked fluid membranes. *J. Phys. II France.* 4:805–817.

Pearson, L. T., J. Edelman, and S. I. Chan. 1984. Statistical mechanics of lipid membranes, protein correlation functions and lipid ordering. *Biophys. J.* 45:863–871.

Pearson, L. T., B. A. Lewis, D. M. Engelman, and S. I. Chan. 1983. Pair distribution functions of bacteriorhodopsin and rhodopsin in model bilayers. *Biophys. J.* 43:167–174.

Sackmann, E. 1994. Membrane bending energy concept of vesicle- and cell-shapes and shape-transitions. *FEBS Lett.* 346:3–16.

Safran, S. A. 1994. Thermodynamics of Surfaces, Interfaces, and Membranes. Addison-Wesley, Reading, MA.

Safran, S. A., P. Pincus, and D. Andelman. 1990. Theory of spontaneous vesicle formation in surfactant mixtures. *Science.* 248:354–355.